

A trained humanoid robot can perform human-like crossmodal social attention conflict resolution

Di Fu^{1,2,3}, Fares Abawi³, Hugo Carneiro³, Matthias Kerzel³,
Ziwei Chen^{1,2}, Erik Strahl³, Xun Liu^{1,2*}, Stefan Wermter³

¹CAS Key Laboratory of Behavioral Science, Institute of Psychology, Beijing, China

²Department of Psychology, University of Chinese Academy of Sciences, Beijing, China

³Department of Informatics, University of Hamburg, Hamburg, Germany

*To whom correspondence should be addressed; E-mail: liux@psych.ac.cn.

Due to the COVID-19 pandemic, robots could be seen as potential resources in tasks like helping people work remotely, sustaining social distancing, and improving mental or physical health. To enhance human-robot interaction, it is essential for robots to become more socialised, via processing multiple social cues in a complex real-world environment. Our study adopted a neurorobotic paradigm of gaze-triggered audio-visual crossmodal integration to make an iCub robot express human-like social attention responses. At first, a behavioural experiment was conducted on 37 human participants. To improve ecological validity, a round-table meeting scenario with three masked animated avatars was designed with the middle one capable of performing gaze shift, and the other two capable of generating sound. The gaze direction and the sound location are either congruent or incongruent. Masks were used to cover all facial visual cues other than the avatars' eyes. We observed that

the avatar's gaze could trigger crossmodal social attention with better human performance in the audio-visual congruent condition than in the incongruent condition. Then, our computational model, GASP, was trained to implement social cue detection, audio-visual saliency prediction, and selective attention. After finishing the model training, the iCub robot was exposed to similar laboratory conditions as human participants, demonstrating that it can replicate similar attention responses as humans regarding the congruency and incongruency performance, while overall the human performance was still superior. Therefore, this interdisciplinary work provides new insights on mechanisms of crossmodal social attention and how it can be modelled in robots in a complex environment.

Summary

An iCub robot can express human-like social attention responses in a gaze-triggered audio-visual crossmodal meeting scenario.

Introduction

Robots are increasingly becoming an integral part of daily life in today's society. Not only based on the recent outbreak of the COVID-19 pandemic, humans are experiencing remote work and social distancing on a regular basis. Robots play an assistive role in mitigating the secondary effects of COVID-19 and other infectious disease outbreaks by assisting social distancing, improving mental health, remote education, manufacturing and economic recovery (1, 2). The need for such solutions encourages the design of socially functional robots capable of meeting more significant challenges and difficulties. For example, researchers have developed robots which can conduct viral nucleic acid detection (3), hotel service (4), masked facial recogni-

tion (5), among many other tasks. Robots are no longer associated only with basic mechanical attributes, having nowadays also some social attributes capable of processing multimodal social information and adapting to the human social environment. Currently, there are computational models capable of processing information cues this way (6, 7). However, their practical and commercial applications in humanoid robots are still scarce, making this study an important step towards building humanoid agents which can better attend to and interact with people. Therefore, it is crucial to make robots process information cues from a complex social environment appropriately and efficiently to serve society better. Furthermore, in order to improve the interaction between humans and robots, it is desirable that robots have similar behavioural performance as humans in processing information cues.

For humans, social attention is the fundamental function of sharing and conveying information with other agents, contributing to the functional development of social cognition (8). Social attention allows humans to capture and analyse others' facial expressions, voice, gestures, and social behaviour quickly in order to participate in social interaction and adapt within a society (9, 10). Furthermore, this social function enables the recognition of others' intents, and the capture of relevant occurrences in the environment (e.g., frightening stimuli, novel stimuli, reward stimuli, etc) (11). The neural substrates underlying social attention are brain regions responsible for processing social cues and encoding human social behaviour, including orbital frontal and middle frontal gyrus, superior temporal gyrus, temporal horn, amygdala, anterior precuneus lobe, temporoparietal junction, anterior cingulate cortex, and insula (11, 12). From the developmental perspective, infants' attention to social cues helps them quickly learn how to interact with others, learn language, and build social relationships (13). However, dysfunction of social attention may lead to mental disorders (14) and poor social skills (15). For example, infants with Autism Spectrum Disorder (ASD) are born with less attention to social cues, an inability to track the sight of others, and a fear of looking directly at human faces (16). This re-

sults in their failure to understand others' behavioural intentions and to engage in typical social interactions. At present, the understanding of the social attention developmental mechanisms is still in its infancy with many questions remaining. Exploring these scientific questions will be significant for understanding mechanisms of interpersonal social behaviour and for developing clinical interventions for individuals diagnosed with ASD.

One of the most critical manifestations of social attention is the ability to follow others' eye gaze and respond with appropriate behaviours (17). Eye gaze is proven to have higher social saliency and prioritisation than other social cues (9) since it gives a person the direction of another person's gaze and intention (18). Gaze following is supposed to be the foundation of more sophisticated social and cognitive functions like the theory of mind, social interaction, and survival strategies formed by evolution (9, 19). Even infants can track the eye gaze of their parents while they are still unable to speak and walk (20, 21). Moreover, gaze following contributes significantly to the language development of infants (22). Psychological studies use the modified Posner cueing task (23) or named gaze-cueing task (24) to study reflexive attentional orienting generated by the eye gaze. During the task, the human eye gaze is presented as the visual cue in the middle of the screen, followed by a peripheral target, which could be spatially congruent (e.g., a right-shift eye gaze followed by a square frame or a Gabor patch shown on the right side of the screen) or incongruent. However, studying visual attention alone is not enough to reveal how humans can quickly recognise social and emotional information conveyed by others while being in an environment and using multiple sensory modalities (25). Being able to select information from a common external source across different modalities allows humans to detect crucial information such as life threats, survival-related information, *etc* (26, 27). Therefore, several studies conducting a crossmodal gaze-cueing task demonstrate the reflexive attentional effect of the visual cue on the auditory target (28, 29). However, most of those studies use static eye gaze shift images as the visual cue to trigger the observer's social

attention (26, 30), which is not the real and natural way humans shift their eye gaze.

The current study adopted a dynamic social gaze-cueing paradigm similar to those frequently used in gaze-cueing experiments to test the effect of eye gaze cues on auditory target detection. Pursuing realistic experimental scenarios, we used the avatar stimuli and meeting scenario published in our previous work on crossmodal spatial attention localisation tasks (31, 32). In these two studies, a 4-avatar meeting scenario experiment with lip movement and arm movement as visual cues was conducted on human participants. Our previous findings show that lip movement is more salient than arm movement, showing a stronger visual bias on auditory target localisation. This is due to the strong natural association between mouth and voice generation of humans. Furthermore, previous research also reveals that head orientation is also a crucial social cue for triggering the reflexive attention of the observer (9). In sum, to keep the balance between ecological validity and confounding variables, we adopted a new 3-avatar meeting scenario in the current study. We made the middle avatar shift its eyes while also including a realistic combination of head and slight upper body movement with the same direction of the gaze. To avoid the distracting effect from lip movement, we made all three avatars wear facial masks to cover movement from their noses, mouths and jaws. Due to the COVID-19 pandemic, the use of masks in multi-person social contexts became a norm. It is also a new habit and challenge for humans to identify social intent from eye gaze information while not being able to perceive lip movement. In the current study, human participants reported no unfamiliarity or discomfort with the avatar wearing the mask.

In the current study, an iCub head is capable of predicting human social attention in an audio-visual crossmodal social scenario. Given the research goals and this study, there was no need for the whole iCub robot, but just its head. The ability of predicting human social attention in an audio-visual crossmodal social scenario is granted to the iCub via the use of the audio-visual crossmodal saliency prediction model GASP (Gated Attention for Saliency Predic-

tion) (6). GASP can detect social cues from eye gaze information and sound source localisation, producing feature maps for each of those cues. By prioritising some social cues rather than others through a directed attention module and then sequentially integrating them, GASP is capable of furnishing a fixation density map that resembles the human social attention, allowing for the iCub head to provide human-like responses in the experimental scenario. Studies with meaning maps (33) show that those closely resemble human attention maps (and fixation density maps). Meaning maps, in turn, are generated based on users specifying grid regions that had a high relevance for them, similarly to how humans responded by pressing a key corresponding to a particular region (left or right) that attracted their attention.

The goals of our current study are twofold. First, our study aims to detect human responses in an audio-visual crossmodal social attention scenario with lifelike stimuli to determine the eye gaze orienting effect on sound localisation. Second, our study aims to make humanoid robots mimic the nuances of human behaviour by training the GASP model based on human behaviours and test the robot in similar laboratory conditions. Thus, comparisons between human and iCub responses were performed using congruent and incongruent visual-audio spatial localisation conditions in the gaze-cueing task. We hypothesised that eye gaze would show the reflexive attentional orienting effect on the auditory target for both humans and the robot, resulting in better performance in the congruent condition than in the incongruent one, with shorter reaction time and lower error rates. The robot would have worse performance than humans and might show larger Stimulus-Response Compatibility effects than humans because of the task being considerably complex for a neurorobotic model, given its crossmodality and the use of synthetic, although realistic, inputs (31). By processing human social cues and interpreting human intention, our study aims to make humanoid robots more collaborative with humans and better serve society.

Human behavioural experiment Participants ($N = 37$) sat positioned 55 centimetres from the desktop screen at a desk and wore a headphone, as depicted in Figure 1a. In the task, participants were presented to the trial scenario with three avatars wearing face masks, as illustrated in Figure 1c.

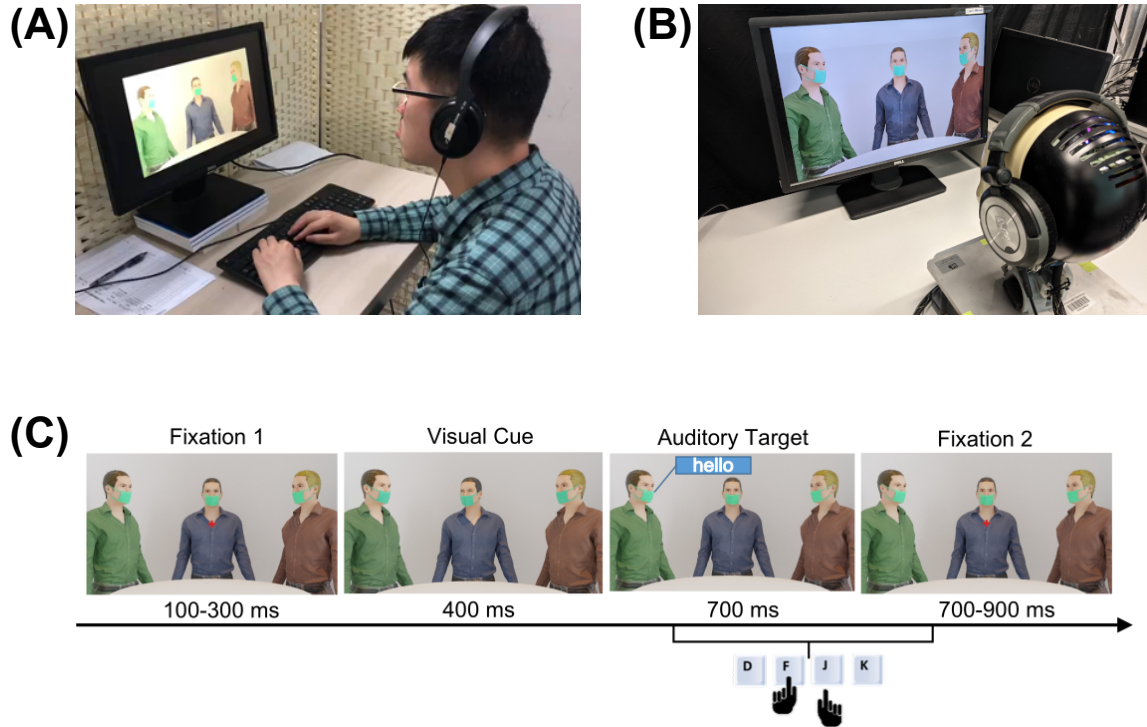


Figure 1: Audio-Visual gaze-cueing social attention task. **A.** Human participant engaging in the formal test with a headphone to hear the auditory stimulus and a keyboard to respond; **B.** The iCub robot engaging in the test with a headphone to get the auditory input and responding to the target by moving its eyeballs (see Figure 4); **C.** Schematic illustration of one trial.

In each trial, the participants were presented with an auditory target, consisting of an utterance (“hello”) originating from one of the peripheral avatars. Since all the avatars in the current experimental scenario wear facial masks, participants could not see any lip or jaw movement from the avatar faces. In the trial, a visual cue could also be provided before the auditory cue. In that case, the central avatar would shift its eye gaze towards one of the other avatars, as well

as synchronously shifting its head and upper body into the same direction. In case a visual cue is not provided, the central avatar stands still looking directly towards the human participant. In summary, there are three distinct directions of the visual cue (left, right and centre), and two of the auditory target localisation (left and right). Thus, three audio-visual crossmodal congruence conditions arise from this experiment: congruent (the visual cue indicates the region where the auditory target is), incongruent (the visual cue indicates the region opposite to that where the auditory target is) and neutral (no visual cue is provided). The generation of visual cues and auditory targets was done to guarantee that every human participant was exposed to the same amount of each crossmodal congruence condition. During the task, the participants were asked to determine as soon and as accurately as possible whether the auditory stimulus originated from the avatar at the left or the one at the right.

Reaction time (RT) and error rates (ER) were analysed as human response indices. For the RT analysis, error trials and trials with RTs shorter than 200 milliseconds, as well as those with RTs beyond 3 standard deviations above or below the mean, were not included, which corresponds to 2.42% of the data being removed. To examine the Stimulus-Response Compatibility (SRC) effects of the audio-visual crossmodal conflict task, one-way repeated measures analysis of variance (ANOVA) were used to test differences in participants' responses under the three congruence conditions (congruent, incongruent and neutral). All post hoc tests in the current study used Bonferroni correction.

iCub experiment To replicate the experiments with human participants as closely as possible for the iCub head, some technical adjustments proved necessary. First, the iCub head was placed at a distance of approximately 30 centimetres from a 24-inch monitor (1920×1200 pixel resolution), as depicted in Figure 1b. This distance is, however, shorter than the 55 centimetres distance the human participants stood from the desktop screen. The distance reduction was

performed so that the iCub’s field of vision covers a larger portion of the monitor. Since the robot lacks a foveated view, the attention is distributed uniformly to all visible regions, causing the robot to attend to irrelevant environmental changes or visual distractors. Second, the previous robot eye fixation position needed to be retained as a starting point for the next trial, as a means to provide scenery variations to the model. This approach closely resembles the human experiment, by intending to simulate a memory mechanism, as the one observed in humans. Direct light sources also needed to be switched off to avoid glare. Once the experimental setup was ready, the pipeline started the video playback in fullscreen mode, simultaneously capturing a 30-frames segment of the video using a single iCub camera¹ along with one-second audio recordings from each microphone² mounted on the iCub’s ears.

In the current study, the iCub head made responses to the auditory target by shifting its eyeballs. This is different from how human participants responded. This difference could lead to systematic differences in RT, therefore the RT of the robot was not measured nor analysed. Nevertheless, it is worth noticing that even though humans and the robot respond differently to a trial, the task they perform is essentially the same. So, ER can be properly measured and analysed as the robot response indices. Like the analysis of human participants, one-way repeated measures ANOVA were used to test the SRC effects of the robot’s response under the three congruence conditions (congruent, incongruent and neutral). All post hoc tests in the current study used Bonferroni correction. Additionally, an independent *t*-test was conducted to compare the difference of SRC effects between humans and the robot. The SRC effect was measured by subtracting congruent responses from incongruent responses.

¹<http://wiki.icub.org/wiki/Cameras>

²<http://wiki.icub.org/wiki/Microphones>

Results

Human behavioural experiment

Reaction time A repeated measures ANOVA with a Greenhouse-Geisser correction showed that participants' RT differed significantly between different congruence conditions, $F(2, 34) = 24.19, p < .001, \eta_p^2 = .40$ (see Figures 2a and 2b). Post hoc test showed that participants responded significantly faster under the congruent condition (mean \pm SE = 466.25 ± 14.92 ms) than both incongruent condition (mean \pm SE = 485.12 ± 14.82 ms, $p < .001$) and neutral condition (mean \pm SE = 485.11 ± 14.80 ms, $p < .001$). However, the difference between incongruent and neutral condition was not significant, $p > .05$.

Error rates A repeated measures ANOVA with a Greenhouse-Geisser correction showed that participants' ER differed significantly between different congruence conditions, $F(2, 34) = 5.69, p < .05, \eta_p^2 = .14$ (see Figures 2c and 2d). Post hoc test showed that participants presented significantly lower ER under the congruent condition (mean \pm SE = $.02 \pm .002$) than incongruent condition (mean \pm SE = $.03 \pm .004$), $p < .01$. However, there was no statistical significance in the difference between the neutral condition (mean \pm SE = $.02 \pm .003$) and both other congruence conditions, $p > .05$ in both cases.

iCub experiment

Error rates A repeated measures ANOVA with a Greenhouse-Geisser correction showed that the robot's ER differed significantly between different congruence conditions, $F(2, 34) = 8.02, p < .01, \eta_p^2 = .18$ (see Figures 2e and 2f). Post hoc test showed that the robot presented significantly lower ER under the congruent condition (mean \pm SE = $.37 \pm .01$) than incongruent condition (mean \pm SE = $.41 \pm .01$), $p < .01$. However, there was no statistical significance in

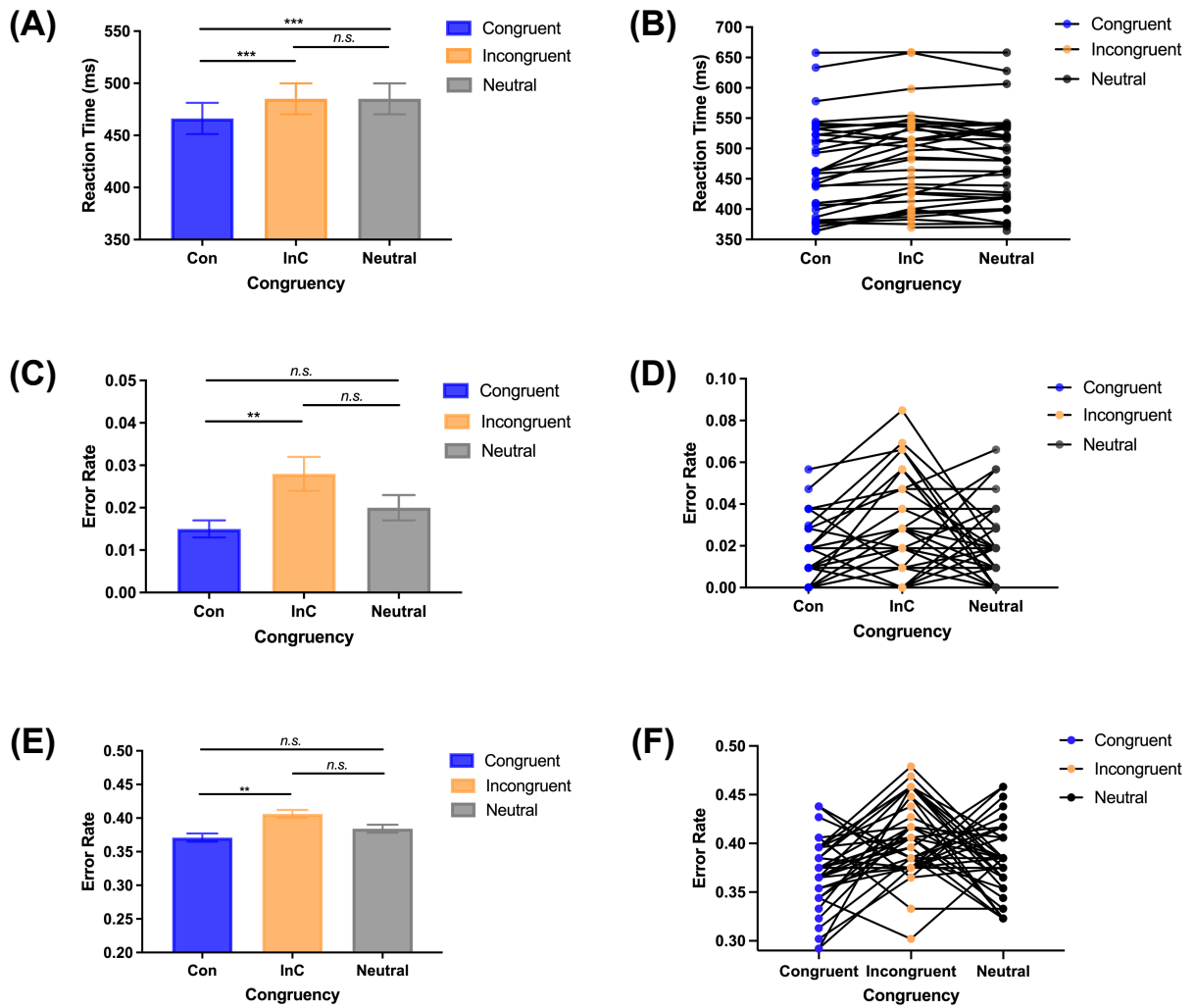


Figure 2: **A.** RT of human participants under different congruence conditions – Group level; **B.** RT of human participants under different congruence conditions – Individual level; **C.** ER of human participants under different congruence conditions – Group level; **D.** ER of human participants under different congruence conditions – Individual level; **E.** ER of the iCub under different congruence conditions – Group level; **F.** ER of the iCub under different congruence conditions – Individual level. * denotes $.01 < p < .05$, ** $.001 < p < .01$, *** $p < .001$, and n.s. denotes no significance.

the difference between the neutral condition (mean \pm SE = $.38 \pm .01$) and both other congruence conditions, $p > .05$ in both cases.

Human-Robot comparison Results of the t -test displayed that the robot showed significantly larger SRC effect (mean \pm SE = $.04 \pm .001$) than humans (mean \pm SE = $.01 \pm .01$), $t(72) = 2.35$, $p < .05$ (see Figure 3).

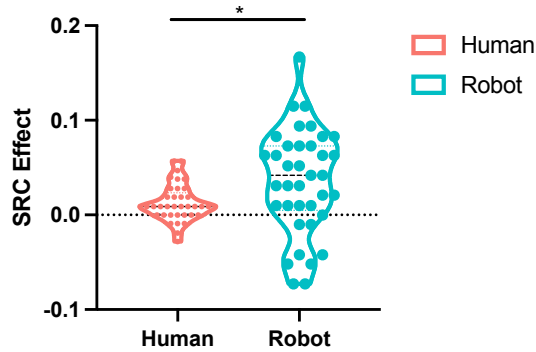


Figure 3: SRC effects comparison between humans and the robot. * denotes $.01 < p < .05$, ** $.001 < p < .01$, *** $p < .001$, and n.s. denotes no significance.

Discussion

Our current neurorobotic study investigated human attentional response and modelled the human-like response with the humanoid iCub robot head in an audio-visual crossmodal social attention meeting scenario. According to the research goals, the main findings of the current study are also twofold. First, in line with previous crossmodal social attention research (34, 35), our study showed that the visual cue direction enhances the detection of the following auditory target occurring in the same direction although from a different modality. Notably, in the current study, a dynamic gaze shift with corresponding head and upper body movements is used as visual cue stimuli. It replicated the previous findings by studies using static eye gaze (15, 30), showing a robust reflexive attentional orienting effect. More specifically, human participants showed longer RT and higher ER under the audio-visual incongruent condition than the congruent one. Some previous research found that eye gaze has stronger attentional orienting effect than simple experimental stimuli (e.g. arrows) (36, 37). Although we did not have any conditions using

arrows as visual cues in our current study, we demonstrated that realistic and dynamic social cues could have a similar effect in a human crossmodal social attention behavioral study. Second, results from the iCub response demonstrated a successful human-like simulation. With the GASP model, the iCub robot was able to trigger similar attentional patterns as humans, even in a complex crossmodal scenario. At last, the statistical comparison of the SRC effects between humans and the iCub showed that the robot experienced a larger conflict effect than humans.

In the human experiment, corresponding to our hypotheses, social cues that triggered social attention were extended to multiple modalities. Our results support the nature of social gaze cueing, and the view of stimulus-driven shifts of auditory attention might be mediated by other modality information (17). Furthermore, different from previous gaze-cueing experiments (34), we added a neutral condition to be more natural for the meeting scenario. At the same time, the neutral condition was regarded as the baseline compared with other conditions. For the neutral condition, participants only saw a static meeting scenario without any dynamic social visual cues before the auditory target came out. Since there was no conflict between audio-visual stimuli in the neutral condition, we assumed there should be no difference between congruent and neutral conditions. However, surprisingly, experiment results showed that participants had significantly longer RT under the neutral condition than under the congruent condition. However, no significant difference in RT between neutral and incongruent conditions was found. These counterintuitive results could be due to human participants' expectations on the direction of the visual cue during each experiment trial. ER showed a reasonable result that the neutral condition had higher ER than congruent condition and lower ER than incongruent condition, but without any significant difference. Taken together, a neutral condition without gaze cue lowers the response speed, while not facilitating the following auditory target detection.

The iCub experiment reveals that, similarly to humans, the robot's response accuracy is significantly better ($p < .01$) in a congruent condition than in an incongruent one. This similarity

is further corroborated by the lack of significant difference ($p > .05$) in both humans' and the robot's ER in the neutral condition compared to either of the other conditions (cf. Figures 2c and 2e). Notably, in the current study, we did not compare ER from humans and the robot directly under each condition. Because robots do not respond as accurately as humans, lower accuracy is to be expected for robots (38). However, it is still important to find that the relevant values between incongruent and congruent conditions between humans and the robot are closely related. Although the SRC effect of the robot is significantly larger than for humans, it is reasonable for responses from the robot to have more variants and uncertainty than those of humans. The iCub's ego noise, though very low, still makes audio localisation more challenging than for a human, that could adjust to the visuals of the avatars in the pretrials whereas the iCub could rely solely on its pretrained model. Besides, it is worth noticing that even though human participants responded to the stimuli by pressing the corresponding keys on the keyboard, while the iCub robot responded by shifting its eyeballs, the SRC effects were still replicated with the performances on ER. The robot provides a fixation density map, representing the most likely region a human would tend to fix his/her attention in an audio-visual crossmodal social attention meeting scenario. By providing different degrees of attention to each modality, guaranteeing that all of them would be considered for the determination of the fixation density map, the neurorobotic model is capable of mimicking the human crossmodal attention behaviour. The possibility of making a humanoid robot mimic human attention behaviour is an essential step towards creating robots that can understand human intentions, predict their behaviours, and behave naturally and smoothly in human-robot interactions.

The current study could inspire future studies from multiple areas and perspectives. First, future research could use eye-tracking techniques to collect humans' eye movement data during the social attention task since eye movement is more direct than a keyboard response in an attention task. In addition, the GASP model could also be trained based on humans' eye move-

ment data, which may lead to better accuracy in modelling human behaviour in sound source localisation. This is due to the GASP model being originally trained by human eye movement watching natural videos (6). Second, to make the experimental design more diverse and realistic, future studies could utilise other social cues from the avatar's face and body. Besides, the experimental design could be enhanced by considering additional factors, such as the emotion and other identity features from the avatars. This could be helpful for target speaker detection, emotion recognition, and sound localisation in future robotic studies. Considering that speaking activity is one key feature in determining which people to look at (39), it seems as an important factor to consider when creating robots that mimic human attention behaviour. Also, the high performance of the most recent in-the-wild active speaker detection models (40–42) indicates their reliability in providing accurate attention maps. Third, our current work and findings can be applied to build social robots to play with children who have ASD and other mental disorders. Previous research has shown that ASD children avoid mutual gaze and other social interaction with humans but not with humanoid robots (43). This is explained as they fear human faces with eye gaze but not humanoid robot faces. Thus, it is possible and meaningful for social robots to help ASD children improve their social functions. Last but not least, the current experiment could be extended to a human-robot interaction scenario, such as replacing avatars with real humans or robots and evaluating responses from human participants and robots (44). There have been several human-robot interaction studies about how humans react to a robot's eye gaze (45–47) or the mutual gaze effect on human's decision making (48, 49). Based on our study, what can be extended, but can also be challenging, is to make robots learn multiperson eye gaze and detect the important target person in real-time during any collaborative task or social scenario with humans.

In conclusion, our interdisciplinary study provides new insights on how social cues trigger social attention in a complex multisensory scenario with realistic and dynamic social cues and

stimuli. We also demonstrated that by predicting the fixation density map, the GASP model triggered the iCub robot to have a human-like response and similar socio-cognitive functions, resolving sensory conflicts within a high-level social context. By combining stimulus-driven information with internal targets and expectations, we hypothesise that these aspects of multisensory interaction should enable current computational models of robot perception to yield robust and flexible social behaviour during human-robot interaction.

Methods and Materials

Participants A total of 37 participants (female = 20) participated in this experiment. Participants aged from 18 to 29 years, with a mean age of 22.89 years. All participants reported that they did not have a history of any neurological conditions (seizures, epilepsy, stroke, etc.), and had either normal or corrected-to-normal vision and hearing. This study was conducted in accordance with the principles expressed in the Declaration of Helsinki. Each participant signed a consent form approved by the Ethics Committee of Institute of Psychology, Chinese Academy of Sciences.

Apparatus, stimuli and procedure Virtual avatars were chosen over recordings of real people, as the experiment requires strict control over the behaviour of the avatar both in terms of timing and exact motion. By using synthetic data as the experimental stimuli, it can be ensured, for instance, that looking to the left and right are exactly symmetrical motions, thus avoiding any possible bias. Moreover, the use of three identical avatars that are only different in terms of clothing colour also alleviates a bias towards individual persons in a real setting. The static basis for the highly-realistic virtual avatars was created in MakeHuman³. Based on these avatar models, a data generation framework for research on shared perception and social cue learning

³<http://www.makehumancommunity.org/>

with virtual avatars (50) (realised in Blender⁴ and Python) creates the animated scenes with the avatars, which are used as the experimental stimuli in this study. The localised sounds are created from a single sound file using a head-related transfer function that modifies the left and right audio channels to simulate different latencies and damping effects for sounds coming from different directions. In our 3-avatar scenario the directions are frontal left and frontal right at 60 degrees, which correspond to the positions where the peripheral avatars stand.

In each trial, at first a fixation cross is shown at the centre of the screen for a short period of time, which could be for a duration of 100, 200 or 300 milliseconds with equal probability. Next, a visual cue is displayed for 400 milliseconds, consisting of an eye gaze shift and the synchronised head and upper body slight shift from the central avatar. In each trial, the central avatar randomly chooses to look at the avatar at the right, at the one at the left, or directly towards the participant, meaning no eye gaze shift at all. Afterwards, either the left or the right avatar says “hello” with a human male voice as the auditory target. This step lasts for 700 milliseconds. Since all the avatars in the current experimental scenario wear facial masks, participants could not see any lip movement or jaw movement from the avatar faces. Finally, another fixation cross is shown at the centre of the screen for 700, 800 or 900 milliseconds, with equal probability, until the end of the trial (cf. Figure 1c for a schematic representation of the trial).

During the task, the participants were asked to determine as soon and precisely as possible whether the auditory stimulus originated from the avatar at the left or the one at the right. Participants made decisions by pressing the keys “F” and “J” on the keyboard, corresponding to the left and right avatars, respectively. Participants’ response during the display of the auditory target and the second fixation were recorded. The stimulus display and the response recording were both under the control of E-prime 2.0⁵.

⁴Free and open source 3D creation suite Blender: <https://www.blender.org/>

⁵Schneider, W., Eschman, A., & Zuccolotto, A. (2002). E-Prime (Version 2.0). [Computer software and

Participants began the experiment by being subjected to 30 practice trials and entered into the formal test after their accuracy of practice trials reached 90%. Each condition was repeated 96 times, with a total of 288 trials separated into 4 blocks. A one-minute rest was offered between each two blocks. The time duration for each trial ranged from 1,900 to 2,300 milliseconds, with the formal test lasting for 12 minutes.

iCub head The iCub robot is a robot developed in the EU project RobotCup with the goal to create an open-source robot platform, especially for research in embodied cognition (51). Its neck has three degrees of freedom for pan, tilt and swing movements and the joints are equipped with absolute position sensors for full head control. The eyes have a common tilt but independent pan to allow vergence movements, resulting in three degrees of freedom. They contain two VGA colour cameras. The head contains two microphones with ear pinna and a loudspeaker. The head used for the experiments (see Figure 4) is a special version with extended audio capabilities, where the fan noise has been reduced and which was equipped with improved microphones (Soundman OKM II).

GASP The process of saliency prediction done by GASP is divided into two stages. The first one, Social Cue Detection (SCD), is responsible for extracting social cue feature maps (FM) from a given image. Figure 5a depicts the architecture of the SCD stage. Given a sequence of images and its corresponding high-level feature maps, the second stage, GASP, then predicts the corresponding saliency region. The architecture of GASP is given by Figure 5b.

In (6), SCD comprises four modules, each responsible for extracting a specific social cue. Those modules encompass gaze following (GF), gaze estimation (GE), facial emotion recognition (FER), and audio-visual saliency prediction (AVSP). For the current task, however, the FER module is not employed because no emotion cues are present in the current research. Also, manual]. Pittsburgh, PA: Psychology Software Tools Inc.

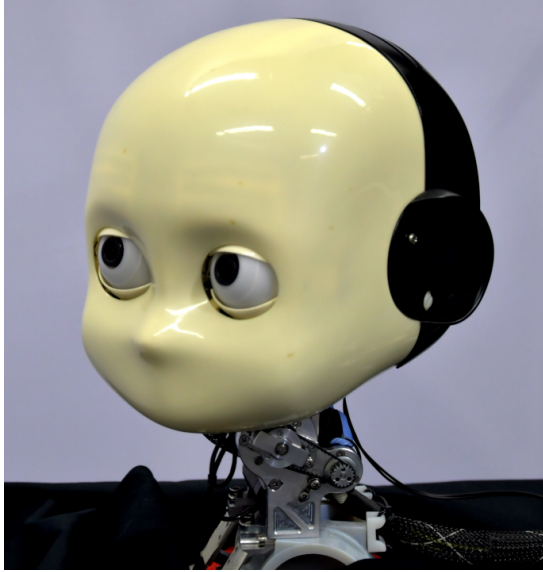


Figure 4: The iCub head

in order to better replicate the experiments done with human participants, the iCub robot would receive auditory stimuli from two sources (one for each of the iCub’s ears). Originally AVSP was implemented to work with monaural data. To allow GASP to work with binaural data, the AVSP module is replaced by a sound source localisation module (SSL), denoted as “SSL model” in Figure 5a, whose architecture is offered in Figure 5c.

GASP uses a video stream as its input, which is split into frames and their corresponding audio signals. For every video frame and corresponding audio signal, SCD extracts the aforementioned high-level feature maps, which are then sent as input to GASP. A direct attention module (DAM) weighs the FM channels as to emphasise those which are more unexpected. Convolutional models further encode those weighted FM channels. In Figure 5b, they are denoted as “Enc.” (for encoder). One can notice that there are as many encoders as there are FM channels, and that each encoder is responsible for encoding a particular feature map. The encoded feature maps of all video frames are then finally integrated via a recurrent extension of the convolutional variant of the gated multimodal unit (GMU) (52). The GMU utilises a gating

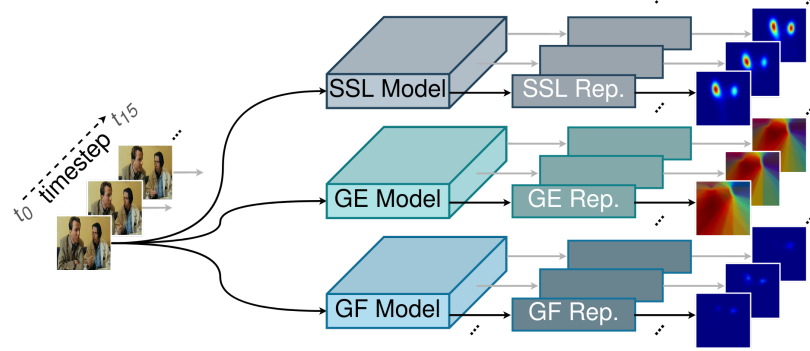
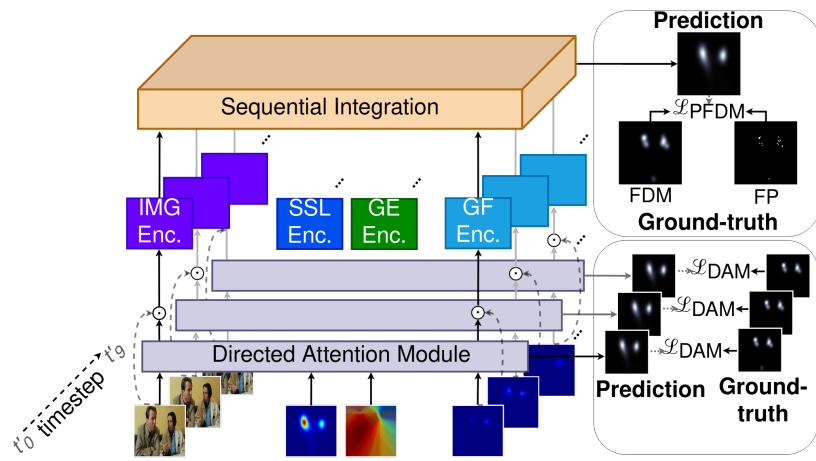
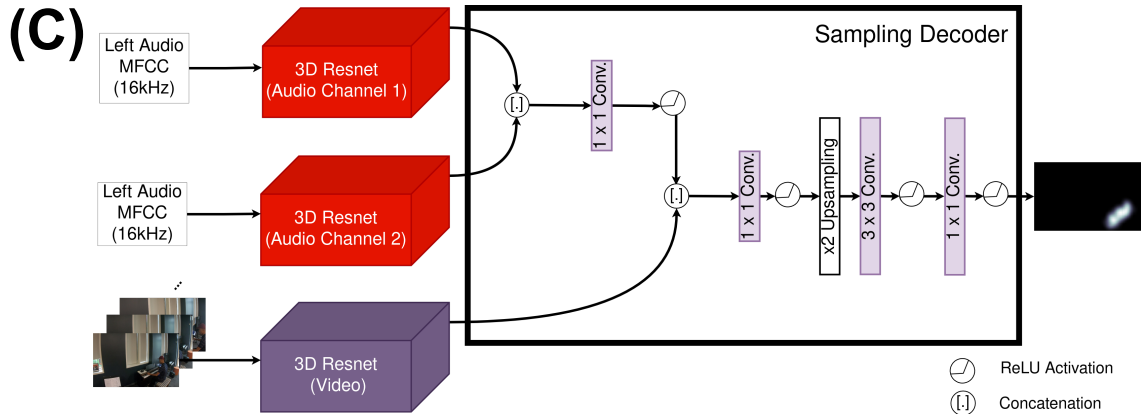
(A)**(B)****(C)**

Figure 5: Architectures of the main structures of GASP: **A.** SCD – Social cue detection; **B.** GASP – Saliency prediction; **C.** Binaural DAVE – Sound source localisation

mechanism to weigh its input features. The convolution addition accounts for the preservation of spatial properties of the input features. The recurrent property of integration unit considers the whole sequence of frames, by performing the gated fusion at every timestep.

For the purpose of this work, the LARGMU (Late Attentive Recurrent Gated Multimodal Unit) is used since it was shown to outperform other GMU-based models (6). Since it is based on the convolution GMU, it preserves the input spatial features. LARGMU’s recurrent nature allows it to integrate those features sequentially. The addition of a soft-attention mechanism based on the convolutional Attentive Long Short-Term Memory (ALSTM) (53) prevents gradients from vanishing as feature sequences get sufficiently large. As the name implies, LARGMU is a late fusion unit, which means that the gated integration is performed after the input channels are concatenated and, in sequence, propagated to the ALSTM.

Binaural DAVE In its paper (6), GASP uses DAVE (Deep Audio-Visual Embedding) (54) for audio-visual saliency prediction. DAVE, however, was originally conceived to work with monaural input. For this research work, DAVE is extended to accept binaural input. Figure 5c presents the structure of this extension. The original monaural DAVE has inputs from one video and one audio stream, which are projected into a feature space by 3D-ResNets (one for each input stream). DAVE concatenates the features output by the 3D-ResNets and via a saliency decoder composed of convolutional and upscaling layers provides the corresponding saliency map.

DAVE’s binaural extension uses a similar rationale, as can be noticed in Figure 5c. The main difference between DAVE and its binaural extension is the use of two audio input streams and, consequently, the use of two 3D-ResNets to process the auditory modality, whose output features are concatenated and then encoded and downsampled by a two-dimensional convolutional layer. This layer is responsible for guaranteeing that the dimension of the feature produced by

that part of the architecture matches that of the feature produced by DAVE’s original audio-stream 3D-ResNet.

DAVE’s pretrained weights are transferred to its binaural extension accordingly. Regarding the pretrained weights of DAVE’s audio-stream 3D-ResNet, they are cloned to both 3D-ResNets associated to binaural DAVE’s left and right audio channels. The 1×1 convolutional layer that encodes the concatenated audio features is initialised using the He normal method (55). During the model training, all model parameters are optimised except for those of the video-stream 3D-ResNet, which are kept frozen throughout the training procedure. The binaural DAVE is trained on a subset of the FAIRplay dataset (56), comprising 500 randomly chosen videos. The FAIRPlay dataset consists of 1,781 video clips of individuals playing instruments in a room. Auditory inputs are binaural and the source location of the sound is provided in the dataset. Even though trials presented to the iCub experiment have a speech signal as the auditory input, this dataset was the closest fit to our needs. Binaural datasets are very scarce and by the time of the experiments only two binaural datasets have been found by the authors. FAIRPlay and one dataset in which speech was used as the auditory input, however the visual part of the dataset consisted of videos recorded with a 360-degrees panoramic camera and in many samples the sound source was located “behind the camera”, which would require us to remove roughly half of the dataset. This reduction would end up making the dataset too small for our needs. Besides, the camera footages were also distorted due to the camera used in the videos. Given those issues, this dataset would not be adequate for fine-tuning binaural DAVE, leading us to FAIRPlay as the most adequate dataset for this task.

Similarly to its monaural counterpart, training binaural DAVE consists of minimising the loss function

$$\mathcal{L}(G, S) = D_{KL}(G \parallel S), \quad (1)$$

where G is the ground truth saliency distribution obtained from fixation density maps, S is the

saliency distribution predicted by the model, and $D_{KL}(G \parallel S)$ is the Kullback-Leibler divergence between those distributions. ADAM optimiser is used for the minimisation during 50 epochs with mini-batches with 64 data set entries.

Applying binaural audio-visual data to GASP The GASP architecture used in the experimental setup consists of the pretrained GASP ablated by removing the FER model. The original AVSP model of FER-ablated GASP is substituted by trained binaural DAVE as a sound source localisation model, with no need to fine-tune GASP. The robustness of GASP regarding its possibility of having its AVSP model changed for another pretrained model with no need of further fine-tuning was attest in (6). GASP kept its high performance on saliency prediction even when its AVSP model was substituted by another pretrained saliency prediction model without the need of fine-tuning. Furthermore, the performance of GASP with the addition of a given pretrained saliency prediction model \mathcal{M} was higher than that of \mathcal{M} alone (6).

GASP receives as input four sequences of data, one sequence of consecutive frames of the original video and three sequences of feature maps, one for each model in the SCD part. For the sake of this experimental work, sequences of size 10 were used (cf. timesteps t'_0 to t'_9 in Figure 5b). The number of frames received as input by each model in SCD varies due to the dissimilar nature of their original specifications. The SSL model receives a sequence of 16 frames as input, and the GE and GF models, each receives a sequence of 7 frames. A more detailed explanation on how the frames are selected based on the timestep being processed is provided in (6). Regarding the audio input, a whole one-second chunk is offered as input to each of the audio 3D-ResNets of the SSL model regardless of the timestep. In this experiment, GASP was embedded in an iCub robot, which, in turn, was subjected to the same series of one-second videos the human participants were. In summary, the one-second chunk used as input to the SSL model’s audio 3D-ResNets consists of the entire audio of an event. Different streams

of audio are sent as input to each of the audio 3D-ResNets depending on where the audio signal originates.

iCub eye movement determination Having the iCub acquired the visual and auditory inputs, the social cue detectors and the sound source localiser extract features from those audio-visual frames. Following the detection and generation of the feature maps, those are propagated to GASP, which, in turn, predicts a fixation density map (FDM) $\mathcal{F}: \mathbb{Z}^2 \rightarrow [0, 1]$, which is displayed in the form of a saliency map for a given frame. The FDM peak $(x_{\mathcal{F}}, y_{\mathcal{F}})$ is determined by calculating

$$(x_{\mathcal{F}}, y_{\mathcal{F}}) = \operatorname{argmax}_{x,y} \mathcal{F}(x, y). \quad (2)$$

The values of $x_{\mathcal{F}}$ and $y_{\mathcal{F}}$, originally in pixels, are then normalised to scalar values $\hat{x}_{\mathcal{F}}$ and $\hat{y}_{\mathcal{F}}$ within the $[-1, 1]$ range, such that

$$\hat{x}_{\mathcal{F}} = \frac{2x_{\mathcal{F}}}{l_x} - 1, \quad (3)$$

$$\hat{y}_{\mathcal{F}} = \frac{2y_{\mathcal{F}}}{l_y} - 1, \quad (4)$$

where l_x and l_y are the lengths of the FDM in the horizontal and vertical axes, i.e., its width and height measured in pixels, respectively. A value of $\hat{x}_{\mathcal{F}} = -1$ represents the leftmost point and $\hat{x}_{\mathcal{F}} = 1$ the rightmost one. Regarding the vertical axis, $\hat{y}_{\mathcal{F}} = -1$ represents the highest point and $\hat{y}_{\mathcal{F}} = 1$ the lowest one.

The robot is actuated to look towards the FDM peak. For simplicity, eye movement is assumed to be independent of the exact camera location relative to the playback monitor. For all experiments, only the iCub eyes were actuated while disregarding microsaccadic movements and vergence effects. The positions the iCub should look at are expressed in Cartesian coordinates while assuming the monitor to be at a distance of 30 centimetres from the image plane. To limit the viewing range of the eyes, $\hat{x}_{\mathcal{F}}$ and $\hat{y}_{\mathcal{F}}$ are scaled down by a factor of 0.3. Those

Cartesian coordinates are then further converted to spherical coordinates θ and ϕ via

$$\theta = \arctan \left(\frac{\hat{x}_{\mathcal{F}}}{0.3\sqrt{1 + \hat{y}_{\mathcal{F}}^2}} \right), \quad (5)$$

$$\phi = \arctan(\hat{y}_{\mathcal{F}}), \quad (6)$$

where θ and ϕ are the yaw and pitch angles, respectively. Those angles are used to actuate the eyes of the iCub such that they pan $\sim 27^\circ$ and tilt $\sim 24^\circ$ at most⁶.

References

1. G.-Z. Yang, *et al.*, Combating COVID-19 – The role of robotics in managing public health and infectious diseases, *Science Robotics* **5** (2020).
2. B. Scassellati, M. Vázquez, The potential of socially assistive robots during infectious disease outbreaks, *Science Robotics* **5** (2020).
3. S.-Q. Li, *et al.*, Clinical application of an intelligent oropharyngeal swab robot: implication for the COVID-19 pandemic, *European Respiratory Journal* **56** (2020).
4. S. S. Kim, J. Kim, F. Badu-Baiden, M. Giroux, Y. Choi, Preference for robot service or human service in hotels? Impacts of the COVID-19 pandemic, *International Journal of Hospitality Management* **93**, 102795 (2021).
5. M. D. Putro, D.-L. Nguyen, K.-H. Jo, Real-time multi-view face mask detector on edge device for supporting service robots in the covid-19 pandemic, *Asian Conference on Intelligent Information and Database Systems* (Springer, 2021), pp. 507–517.
6. F. Abawi, T. Weber, S. Wermter, GASP: Gated attention for saliency prediction, *Proceedings of the Thirtieth International Joint Conference on Artificial Intelligence, IJCAI-21*,

⁶The iCub can pan its eye within a $[-45^\circ, 45^\circ]$ range and tilt them within a $[-40^\circ, 40^\circ]$ range.

Z.-H. Zhou, ed. (International Joint Conferences on Artificial Intelligence Organization, 2021), pp. 584–591.

7. Z. Bylinskii, *et al.*, Where should saliency models look next?, *European Conference on Computer Vision* (Springer, 2016), pp. 809–824.
8. P. Mundy, L. Newell, Attention, joint attention, and social cognition, *Current Directions in Psychological Science* **16**, 269–274 (2007).
9. S. R. Langton, R. J. Watt, V. Bruce, Do the eyes have it? Cues to the direction of social attention, *Trends in Cognitive Sciences* **4**, 50–59 (2000).
10. I. Laube, S. Kamphuis, P. W. Dicke, P. Thier, Cortical processing of head-and eye-gaze cues guiding joint social attention, *Neuroimage* **54**, 1643–1653 (2011).
11. L. Nummenmaa, A. J. Calder, Neural mechanisms of social attention, *Trends in Cognitive Sciences* **13**, 135–143 (2009).
12. T. Akiyama, *et al.*, Unilateral amygdala lesions hamper attentional orienting triggered by gaze direction, *Cerebral Cortex* **17**, 2593–2600 (2007).
13. H. F. Sperdin, *et al.*, Early alterations of social brain networks in young children with autism, *eLife* **7**, 1–23 (2018).
14. T. Akiyama, *et al.*, Gaze-triggered orienting is reduced in chronic schizophrenia, *Psychiatry Research* **158**, 287–296 (2008).
15. J. Guo, *et al.*, Abnormal alpha modulation in response to human eye gaze predicts inattention severity in children with ADHD, *Developmental Cognitive Neuroscience* **38**, 100671 (2019).

16. A. Senju, M. H. Johnson, Atypical eye contact in autism: models, mechanisms and development, *Neuroscience & Biobehavioral Reviews* **33**, 1204–1214 (2009).
17. S. V. Shepherd, Following gaze: Gaze-following behavior as a window into social cognition, *Frontiers in Integrative Neuroscience* **4**, 5 (2010).
18. A. Frischen, A. P. Bayliss, S. P. Tipper, Gaze cueing of attention: visual attention, social cognition, and individual differences., *Psychological Bulletin* **133**, 694 (2007).
19. S. Baron-Cohen, *Mindblindness: An essay on autism and theory of mind* (MIT press, 1997).
20. T. Farroni, S. Massaccesi, D. Pividori, M. H. Johnson, Gaze following in newborns, *Infancy* **5**, 39–60 (2004).
21. S. Jessen, T. Grossmann, Unconscious discrimination of social cues from eye whites in infants, *Proceedings of the National Academy of Sciences* **111**, 16208–16213 (2014).
22. R. Brooks, A. N. Meltzoff, The development of gaze following and its relation to language, *Developmental Science* **8**, 535–543 (2005).
23. M. Posner, Y. Cohen, *Attention and performance X: Control of language processes* (Psychology Press, London, United Kingdom, 1984), pp. 531–556.
24. C. K. Friesen, A. Kingstone, The eyes have it! Reflexive orienting is triggered by nonpredictive gaze, *Psychonomic Bulletin & Review* **5**, 490–495 (1998).
25. L. Battich, M. Fairhurst, O. Deroy, Coordinating attention requires coordinated senses, *Psychonomic Bulletin & Review* pp. 1–13 (2020).
26. R. Newport, S. Howarth, Social gaze cueing to auditory locations, *Quarterly Journal of Experimental Psychology* **62**, 625–634 (2009).

27. D. Fu, *et al.*, What can computational models learn from human selective attention? A review from an audiovisual unimodal and crossmodal perspective, *Frontiers in Integrative Neuroscience* **14**, 10 (2020).
28. D. Doruk, *et al.*, Cross-modal cueing effects of visuospatial attention on conscious somatosensory perception, *Heliyon* **4**, e00595 (2018).
29. R. K. Maddox, D. A. Pospisil, G. C. Stecker, A. K. Lee, Directing eye gaze enhances auditory spatial cue discrimination, *Current Biology* **24**, 748–752 (2014).
30. P. Nuku, H. Bekkering, When one sees what the other hears: Crossmodal attentional modulation for gazed and non-gazed upon auditory targets, *Consciousness and Cognition* **19**, 135–143 (2010).
31. G. I. Parisi, *et al.*, A neurorobotic experiment for crossmodal conflict resolution in complex environments, *2018 IEEE/RSJ International Conference on Intelligent Robots and Systems (IROS)* (IEEE, 2018), pp. 2330–2335.
32. D. Fu, *et al.*, Assessing the contribution of semantic congruency to multisensory integration and conflict resolution, *IROS 2018 Workshop on Crossmodal Learning for Intelligent Robotics* (IEEE, 2018).
33. J. M. Henderson, T. R. Hayes, Meaning-based guidance of attention in scenes as revealed by meaning maps, *Nature Human Behaviour* **1**, 743–747 (2017).
34. P. Nuku, H. Bekkering, Joint attention: Inferring what others perceive (and don't perceive), *Consciousness and Cognition* **17**, 339–349 (2008).
35. S. Soto-Faraco, S. Sinnott, A. Alsius, A. Kingstone, Spatial orienting of tactile attention induced by social cues, *Psychonomic Bulletin & Review* **12**, 1024–1031 (2005).

36. C. K. Friesen, J. Ristic, A. Kingstone, Attentional effects of counterpredictive gaze and arrow cues, *Journal of Experimental Psychology: Human Perception and Performance* **30**, 319 (2004).

37. J. Ristic, A. Wright, A. Kingstone, Attentional control and reflexive orienting to gaze and arrow cues, *Psychonomic Bulletin & Review* **14**, 964–969 (2007).

38. J. Wang, J. Wang, K. Qian, X. Xie, J. Kuang, Binaural sound localization based on deep neural network and affinity propagation clustering in mismatched HRTF condition, *EURASIP Journal on Audio, Speech, and Music Processing* **2020**, 1–16 (2020).

39. M. Xu, Y. Liu, R. Hu, F. He, Find who to look at: Turning from action to saliency, *IEEE Transactions on Image Processing* **27**, 4529–4544 (2018).

40. J. Roth, *et al.*, AVA-ActiveSpeaker: An audio-visual dataset for active speaker detection, *ICASSP 2020 - 2020 IEEE International Conference on Acoustics, Speech and Signal Processing (ICASSP)* (2020), pp. 4492–4496.

41. H. Carneiro, C. Weber, S. Wermter, FaVoA: Face-Voice association favours ambiguous speaker detection, *Proceedings of the 30th International Conference on Artificial Neural Networks (ICANN 2021)*, I. Farkaš, P. Masulli, S. Otte, S. Wermter, eds., ENNS (Springer Nature, 2021), vol. LNCS 12891 of *Lecture Notes in Computer Science*, pp. 439–450.

42. O. Köpüklü, M. Taseska, G. Rigoll, How to design a three-stage architecture for audio-visual active speaker detection in the wild, *Proceedings of the IEEE/CVF International Conference on Computer Vision (ICCV)* (2021), pp. 1193–1203.

43. B. Scassellati, H. Admoni, M. Matarić, Robots for use in autism research, *Annual Review of Biomedical Engineering* **14**, 275–294 (2012).

44. A. Andriella, *et al.*, Do I have a personality? Endowing care robots with context-dependent personality traits, *International Journal of Social Robotics* pp. 1–22 (2020).
45. N. Pfeifer-Lessmann, T. Pfeifer, I. Wachsmuth, An operational model of joint attention-timing of gaze patterns in interactions between humans and a virtual human, *Proceedings of the Annual Meeting of the Cognitive Science Society* (2012), vol. 34.
46. H. Admoni, B. Scassellati, Social eye gaze in human-robot interaction: a review, *Journal of Human-Robot Interaction* **6**, 25–63 (2017).
47. C. Willemse, S. Marchesi, A. Wykowska, Robot faces that follow gaze facilitate attentional engagement and increase their likeability, *Frontiers in Psychology* **9**, 70 (2018).
48. K. Kompatsiari, F. Ciardo, V. Tikhanoff, G. Metta, A. Wykowska, It's in the eyes: The engaging role of eye contact in HRI, *International Journal of Social Robotics* **13**, 525–535 (2021).
49. M. Belkaid, K. Kompatsiari, D. De Tommaso, I. Zablith, A. Wykowska, Mutual gaze with a robot affects human neural activity and delays decision-making processes, *Science Robotics* **6**, eabc5044 (2021).
50. M. Kerzel, S. Wermter, Towards a data generation framework for affective shared perception and social cue learning using virtual avatars, *Workshop on Affective Shared Perception, ICDL 2020*, IEEE International Conference on Development and Learning (2020).
51. G. Metta, G. Sandini, D. Vernon, L. Natale, F. Nori, The iCub humanoid robot: An open platform for research in embodied cognition, *Proceedings of the 8th Workshop on Performance Metrics for Intelligent Systems*, PerMIS '08 (Association for Computing Machinery, New York, NY, USA, 2008), pp. 50–56.

52. J. Arevalo, T. Solorio, M. M. y Gómez, F. A. González, Gated multimodal networks, *Neural Computing and Applications* **32**, 10209–10228 (2020).

53. M. Cornia, L. Baraldi, G. Serra, R. Cucchiara, Predicting human eye fixations via an LSTM-based saliency attentive model, *IEEE Transactions on Image Processing* **27**, 5142–5154 (2018).

54. H. R. Tavakoli, A. Borji, J. Kannala, E. Rahtu, Deep audio-visual saliency: Baseline model and data, *ACM Symposium on Eye Tracking Research and Applications*, ETRA '20 Short Papers (Association for Computing Machinery, New York, NY, USA, 2020), pp. 1–5.

55. K. He, X. Zhang, S. Ren, J. Sun, Delving deep into rectifiers: Surpassing human-level performance on ImageNet classification, *Proceedings of the 2015 IEEE International Conference on Computer Vision (ICCV)*, ICCV '15 (IEEE Computer Society, USA, 2015), pp. 1026–1034.

56. R. Gao, K. Grauman, 2.5D visual sound, *Proceedings of the IEEE/CVF Conference on Computer Vision and Pattern Recognition (CVPR)* (2019), pp. 324–333.

Acknowledgments

Funding: This work was supported by the National Natural Science Foundation of China (NSFC, No. 62061136001), the German Research Foundation (DFG) under project Transregio Crossmodal Learning (TRR 169). D.F. is funded by the Office of China Postdoctoral Council.

Author contributions: D.F., X.L., and S.W. designed the experiment. D.F. and Z.C. collected the human data. F.A. conducted the computational modelling and robotic experiment. D.F. analysed the data. M.K. developed the framework for generating the experimental stimuli. M.K. and E.S. contributed to the experimental setup and stimuli generation. D.F., H.C., F.A., and

M.K. wrote the manuscript. All authors contributed to improve the manuscript. **Competing interest:** The authors declare no competing interests. We especially thank Dr. Cornelius Weber, Dr. Zhong Yang, Dr. Guochun Yang, and Guangteng Meng for their improvement of the experimental design and the manuscript.

Supplementary materials

Materials and Methods

The example of experimental stimuli and videos for both human data and the iCub robot data collection can be downloaded under this link:

https://www.informatik.uni-hamburg.de/WTM/videos/Fu_et_al_2021.zip.

Data Availability Statement

The human and the iCub response data can be find under this link:

<https://osf.io/fbncu/>.